Vol 13 No 6, June 2004
1009-1963/2004/13(06)/0918-06

Chinese Physics

© 2004 Chin. Phys. Soc.
and IOP Publishing Ltd

Crystallographic and magnetic structures of $Pr_6Fe_{13}Ge$ studied by powder neutron diffraction

Wang Fang-Wei(王芳卫)[a)b)†], Zhang Pan-Lin(张泮霖)[a)],
Shen Bao-Gen(沈保根)[a)], and Yan Qi-Wei(严启伟)[a)]

[a)] *State Key Laboratory of Magnetism, Institute of Physics and Centre for Condensed Matter Physics, Chinese Academy of Sciences, Beijing* 100080, *China*

[b)] *Leon Brillouin Laboratory, CEA/Saclay,* 91191 *Gif sur Yvette, France*

(Received 20 May 2003; revised manuscript received 30 December 2003)

Crystallographic and magnetic structures of $Pr_6Fe_{13}Ge$ have been investigated by high-resolution powder neutron diffraction in the temperature range of 10–300 K. The magnetic structure consists of ferromagnetic Pr_6Fe_{13} slabs that alternate antiferromagnetically, along c, with the next Pr_6Fe_{13} slab separated by a non-magnetic Ge layer. The magnetic moments lie within the ab-planes. The propagation vector of this structure is k=(001) with respect to the conventional reciprocal lattice of the I-centred structure. However, the temperature-dependence of neutron-scattering intensity of the (110) Bragg peak, very similar to the temperature-dependent magnetization measured by SQUID magnetometer, indicates that a small c-axis ferromagnetic component should be added to the above antiferromagnetic model.

Keywords: neutron diffraction, magnetic configuration, $Pr_6Fe_{13}Ge$
PACC: 6112D, 7530

1. Introduction

Rare-earth-iron intermetallic compounds $R_6Fe_{13}X$ (where R=light rare-earth, X=Si, Ge, Sn, Cu, Ag, Al, Ga etc.) have been observed in the sintered Nd–Fe–B magnets as secondary phases, which significantly affect the coercivity and the corrosion protection.[1−4] They crystallize in the tetragonal $Nd_6Fe_{13}Si$ structure,[4] or the ordered variant [5] $La_6Co_{11}Ga_3$ (space group: $I4/mcm$) with a relatively complex crystal structure, including two sites $R_1(8f)$, $R_2(16l)$ for the rare-earth, four sites $Fe_1(4d)$, $Fe_2(16k)$, $Fe_3(16l_1)$, $Fe_4(16l_2)$ for iron and a single site $4a$ for the third element X. All magnetic atoms are closely packed up/down the mirror planes (x, y, 0) and (x, y, 1/2), separated by the non-magnetic atoms located on the planes (x, y, 1/4) and (x, y, 3/4). Thus a sandwich structure M/NM/M (Fig.1) is constructed (M: magnetic atom slab; NM: non-magnetic atom layer).

The magnetic properties of this series have been extensively investigated. Due to the complicated, quasi-layered crystal structure and the difficulty to gain a perfect single phase, the reported magnetic behaviours,[6−10] even the transport properties,[11,12] are differ greatly from sample to sample. For example, $Nd_6Fe_{13}Si$ was first reported to be an antiferromagnet with a Néel temperature T_N of 725 K,[4] but later shown to be a ferromagnet with a Curie temperature T_C of 441 K and a compensation temperature of 357 K;[6] and recently it was shown to be an antiferromagnet [7] while the considerable magnetization below 360 K is attributed to the 'contamination' of a very small amount of ferromagnetic secondary phase Nd_2Fe_{17}.

Recently, neutron diffraction [13−15] showed that the magnetic structure, similar to the one proposed by Kajitani *et al*,[8] can be described as below: the moments in M slabs are strongly ferromagnetically coupled with moments lying in the ab-plane, whereas the slabs are antiferromagnetically coupled with the propagation vector $\boldsymbol{k}$=(001), as seen in Fig.1. However, this spin configuration cannot explain the following experimental results: (1) the presence of a zero-field remanent magnetization;[7,16,17] (2) easy c-axis magnetization checked by x-ray diffraction on the

†E-mail: fwwang@aphy.iphy.ac.cn

magnetically aligned Pr-based samples;[16–19] (3) neither easy-plane nor easy-axis magnetization obtained from Mössbauer spectroscopy on the so-called easy-axis magnetically aligned samples.[19,20]

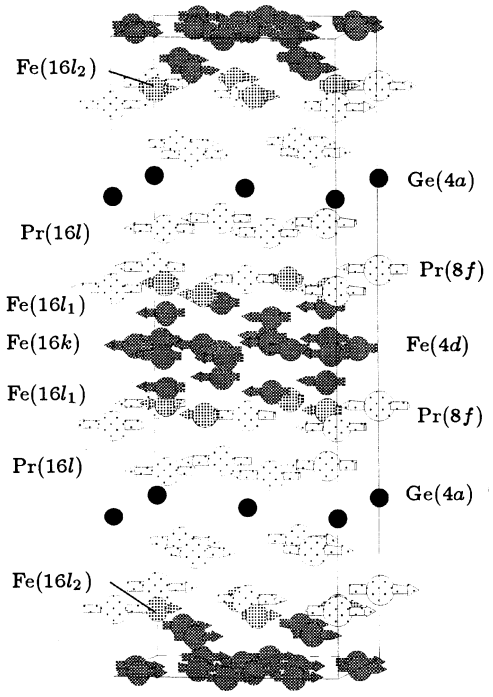


Fig.1. Magnetic structure model of $Pr_6Fe_{13}Ge$ for Rietveld analysis.

In this paper, we report a neutron diffraction study on the crystallographic and magnetic structures of $Pr_6Fe_{13}Ge$ in temperatures ranging from 10 to 300 K. The collinear antiferromagnetic model can be used to refine the collected data, giving a good agreement and a reasonable atomic moment as a function of temperature. However, an additional ferromagnetic component along the c-axis is needed to explain the similarity between the temperature dependence of magnetization and the integrated intensity of the (110) reflection.

2. Experiments

A sample of $Pr_6Fe_{13}Ge$ was prepared by arc melting in an atmosphere of ultra-pure argon gas. The purity of the starting elements was better than 99.9%. The obtained alloy button was sealed in an evacuated quartz tube and annealed at 1000 K for one month. X-ray diffraction shows that the annealed sample crystallizes into a tetragonal $Nd_6Fe_{13}Si$-type structure. Neutron diffraction was carried out on a powder sample in the temperature range of 10–300 K, on a high-resolution neutron diffractometer in HANARO Centre, Korea Atomic Energy Research Institute. An incident beam was monochromatized by a focusing monochromator with the wavelength 0.18437 nm. Data were collected in the range 2θ=0°–140° with a step increment of 0.05°, and analysed by the Rietveld method using the program FullProf.[21] The parameters of the crystal with a tetragonal $Nd_6Fe_{13}Si$-type structure and the model of a magnetic structure [13–15] (Fig.1) were used as the initial input in the refinement.

3. Results

Figure 2 shows the typical neutron diffraction patterns in the range of 2θ=0°–45° taken at temperatures from 10–300 K. The magnetic reflections which are free from overlapping with the nuclear reflections (except (002) peak) are indexed. Due to the neutron optic system (especially the focusing monochromator), the peaks at low angles show a large asymmetry (deviating obviously from the Gaussian profiles), especially for the magnetic (001) reflection and the nuclear (002) reflection. So we cut off the data in the range of 2θ=0°–10° in the Rietveld refinement. This omission would have little affect on the crystallographic parameters. This probably affects the accurate determination of the magnetic moments while the reasonable moments and their temperature dependence have been obtained by the Rietveld refinement.

Figure 3 plots the experimental neutron counts of some typical Bragg peaks as functions of temperature. The (001) reflection, which indicates an antiferromagnetic coupling propagating along the c-axis with moments in ab-plane, is a dominant contribution to the whole magnetic reflections. While its intensity drops sharply with increasing temperatures, it is high enough to consider that the magnetic transition at 482 K is an antiferromagnetism–paramagnetism transition, i.e. T_N=482 K. It can be found that (003) reflection disappears near 75 K while the (205) reflection disappears near room temperature. The intensity of magnetic reflections and their temperature dependence are consistent with previous report, so the model of magnetic structure [13–15] in Fig.1, is adopted directly. Rietveld refinements show that this spin configuration is a good estimation for the collected data. As examples, the refined diffraction patterns at 10, 100 and 300 K are shown in Fig.4, and the corresponding refined parameters are listed in Table 1. It is noteworthy that no secondary phase, such as 2:17-type R-Fe compound or α-Fe,[7,14] was detected.

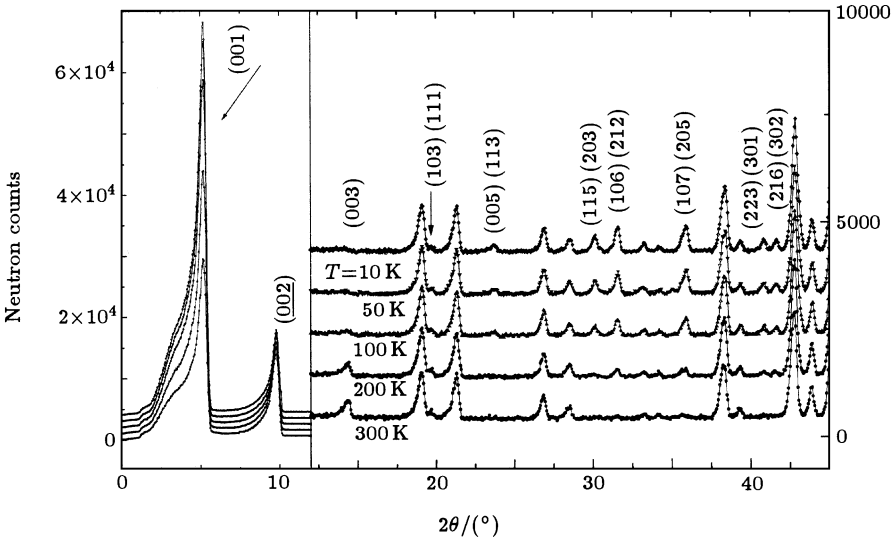


Fig.2. Neutron diffraction pattern of $Pr_6Fe_{13}Ge$ in the range of 0°–40°. The observed magnetic reflections are indicated, and the numbers in brackets are the corresponding index. The data have been offset for clarity.

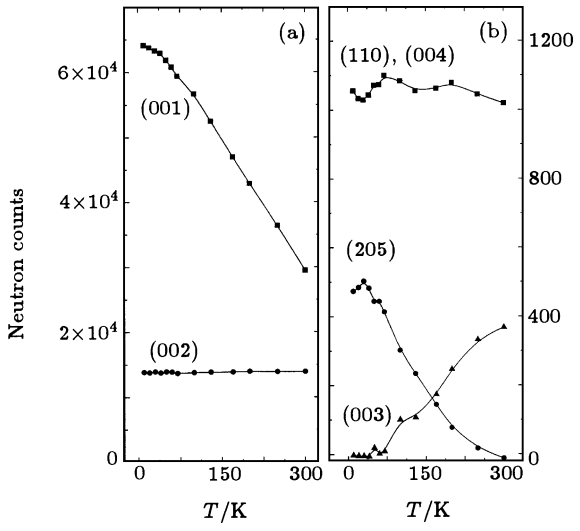


Fig.3. The observed neutron counts for a few special Bragg peaks as functions of temperature (the background has been eliminated). The solid lines are guides for the eyes.

The lattice parameters a and c contract linearly with decreasing temperature with a=0.80907+3.15 × 10^{-6} T (nm) and c=2.2964+ 2.72 × 10^{-5} T (nm) until the parameter c has an anomalous drop near 50 K while a has an expansion (Fig.5). This anisotropic change of lattice parameters coincides with the drop of magnetization at the same temperature, perhaps resulting from the spontaneous magnetostriction.

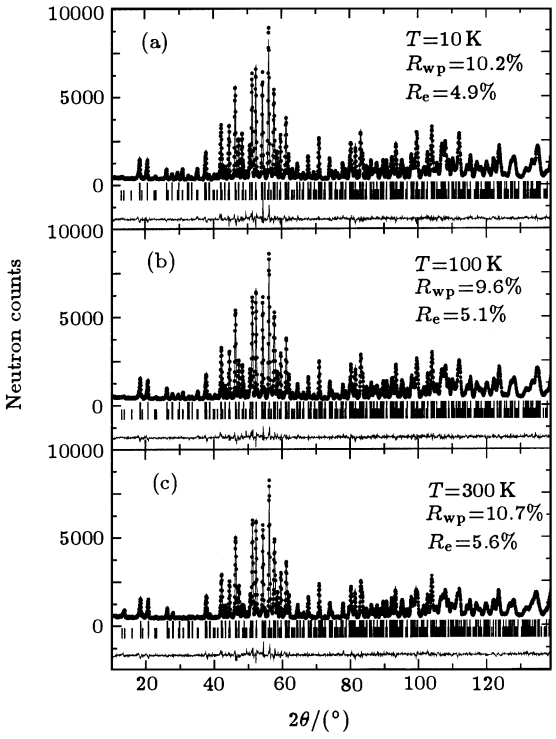


Fig.4. Collected (dots) and calculated (line) patterns of the high resolution powder neutron diffraction at 10, 100 and 300 K. The differences between the observed data and calculated values are also given.

Table 1. Structure parameters and magnetic moments of $Pr_6Fe_{13}Ge$ (space group: $I4/mcm$) derived from the refinement of data collected at 10, 100 and 300 K, respectively. μ is the moment lying in the ab plane. R_n, R_m are the integrated intensity reliability factors of the nuclear and magnetic reflections respectively. R_{wp}, R_e are the weighted pattern factor and the expected weighted pattern factor respectively.

T/K		10	100	300
Pr1 ($8f$)	z	0.1099(2)	0.1101(2)	0.1100(2)
	$B/10^{-4}$nm^2	0.0(1)	0.17(9)	0.6(1)
	μ/μ_B	2.65(5)	2.26(5)	1.01(8)
Pr2 ($16l$)	x	0.1685(3)	0.1686(3)	0.1685(4)
	z	0.1910(1)	0.1906(1)	0.1905(2)
	$B/10^{-4}$nm^2	0.17(6)	0.30(7)	0.9(1)
	μ/μ_B	2.94(3)	2.33(3)	1.06(4)
Fe1 ($4d$)	$B/10^{-4}$nm^2	0.25(5)	0.19(5)	0.1(1)
	μ/μ_B	2.0(1)	2.1(1)	1.7(2)
Fe2 ($16k$)	x	0.0667(2)	0.0662(2)	0.0657(2)
	y	0.2083(2)	0.2079(2)	0.2077(2)
	$B/10^{-4}$nm^2	0.24(4)	0.18(4)	0.16(4)
	μ/μ_B	2.41(5)	2.41(4)	1.79(6)
Fe3 ($16l_1$)	x	0.1788(2)	0.1788(1)	0.1790(2)
	z	0.06080(7)	0.06069(7)	0.0605(1)
	$B/10^{-4}$nm^2	0.25(4)	0.17(4)	0.15(4)
	μ/μ_B	2.36(4)	2.27(4)	1.82(6)
Fe4 ($16l_2$)	x	0.3862(2)	0.3863(1)	0.3864(2)
	z	0.09644(8)	0.09624(8)	0.0956(1)
	$B/10^{-4}$nm^2	0.16(4)	0.08(3)	0.28(4)
	μ/μ_B	2.47(4)	2.37(4)	1.68(7)
Ge ($4a$)	$B/10^{-4}$nm^2	0.12(9)	0.10(8)	0.30(9)
	a/nm	0.80933(1)	0.80939(1)	0.81001(1)
	c/nm	2.2969(4)	2.2991(5)	2.3044(5)
	R_n, R_m/%	3.49, 6.35	3.40, 7.24	4.2, 13.2
	R_{wp}, R_e/%	10.2, 4.89	9.65, 5.08	10.7, 5.6

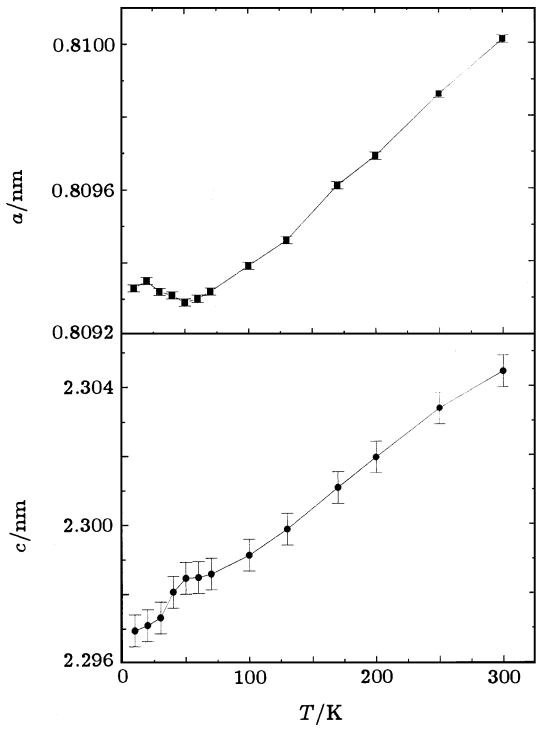


Fig.5. The temperature dependence of the lattice parameters a and c derived from the Rietveld refinement.

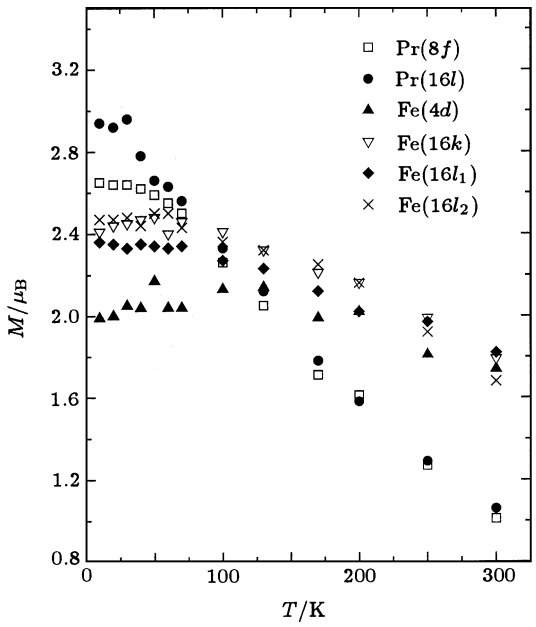


Fig.6. Moments of the magnetic atoms at different sites as functions of temperature derived from the Rietveld refinement under the antiferromagnetic structure are displayed in Fig.1. Maximum error is near 10% for Fe $4d$-site at 300 K, and the minimum is less than 1% for Pr $16l$-site at 10 K. Error bars are omitted from the figure for clarity.

Refined magnetic moments on different sites are shown in Fig.6. At 10 K, the Pr magnetic moments are $M_{\rm Pr}(8f)$=2.65 $\mu_{\rm B}$, $M_{\rm Pr}(16l)$=2.94$\mu_{\rm B}$. They are 17%–18% less than the theoretical magnetic moment of 3.20$\mu_{\rm B}$. The values of Fe atomic moments are located in a reasonable range from $M_{\rm Fe}$ $(4d)$ =1.99 $\mu_{\rm B}$, $M_{\rm Fe}$ $(16l_1)$=2.36$\mu_{\rm B}$, $M_{\rm Fe}$ $(16k)$=2.41$\mu_{\rm B}$ to $M_{\rm Fe}(16l_2)$=2.47$\mu_{\rm B}$. With increasing temperature, all moments have a smooth reduction, and the moments of Pr atoms decrease more quickly than those of Fe atoms.

4. Discussion

Of particular interest is the temperature-dependent intensity (Fig.3(b)) of overlapped (110) and (004) peaks. It is very similar to the temperature dependence of magnetization especially at low temperatures (10–100 K) (in the inset of Fig.7(a)). This similarity seems to indicate its magnetic origin. However, there is no magnetic intensity for (110) and (004) reflections according to the above antiferromagnetic spin configuration. So it is necessary to carefully check the above magnetic structure model again. Since the intensity of the (002) reflection keeps a constant in the whole temperature range, one can reasonably conclude that no change will happen on the (004) peak. Thus this experimental variation of intensity should be attributed to magnetic scattering on (110) reflection, which naturally gives rise to a small ferromagnetic component along the c-axis in addition to the dominant ab-plane antiferromagnetic component.

This argument can be taken to satisfactorily explain all three contradictory experiments summarized in the Introduction. Furthermore, it seems to be supported by the calculation of anisotropy of rare-earth ions using the point charge model.[22] According to the calculation, the second-order crystal field parameter A_{20} of rare-earth ion is estimated to be 1070 K$\cdot a_0^{-2}$ for site 16l and –283 K$\cdot a_0^{-2}$ for site 8f in the series of $R_6Fe_{11}Ga_3$. The competition of opposite magnetocrystalline anisotropy between these two different sites consequently leads to the out-of-plane moments. However, from the dominant strength of anisotropy of the much lower symmetrical 16l site, one can conclude that the moments in $Pr_6Fe_{13}Ge$ prefer to arrange along the c-axis, which is against the experimentally obtained small c-component. Perhaps a relatively strong plane anisotropy of Fe sublattice is responsible for this discrepancy.

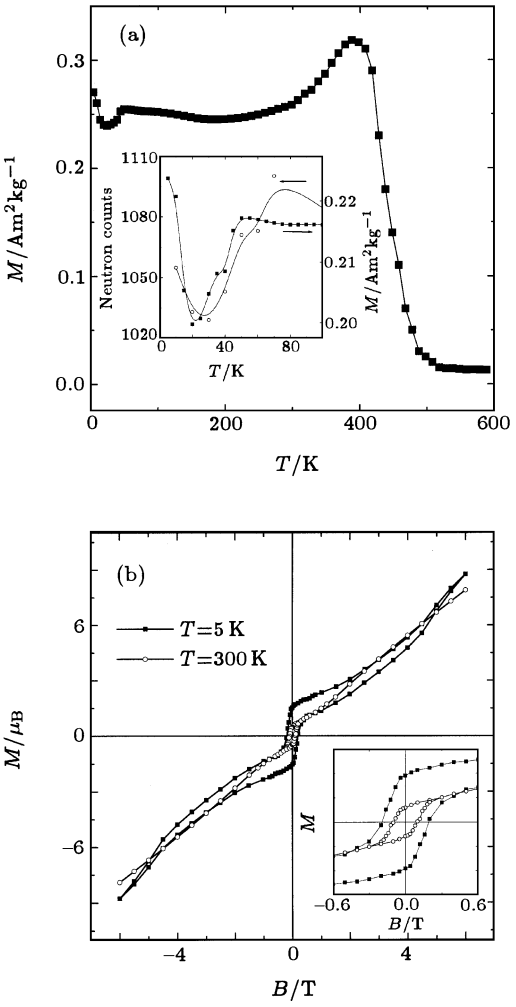


Fig.7. (a) M–T curve of $Pr_6Fe_{13}Ge$ measured under the field of 0.05 T by a commercial SQUID magnetometer MPMS-7 (10–300 K) and a vibrating-sample magnetometer (150–600 K). Inset: the magnetization (solid square) in comparison with neutron diffraction intensity (open circle) of Bragg peaks (110) and (004). (b) Hysteresis at 10 and 300 K. Inset: wider view of the low field part.

We tried to determine this c-axis moment component with the collected data, but did not succeed. The attempted refinement just gives unphysical values for this c-axis ferromagnetic component of all sites with the same order of statistical errors, indicating that this component is too small to be refined by the data of powder neutron diffraction. In fact, this small c-axis component was also displayed by the small zero-field remanent moment in the magnetization loops. In Fig.7(b), one can find that the remanent moment per formula is 0.5$\mu_{\rm B}$ at 300 K and 1.6$\mu_{\rm B}$ at 10 K. They are only 1.7%, 3.3% of the ab-plane component at the corresponding temperatures, with respect to a very small angle (1°–2°) tilted out of the ab-plane.

5. Summary

From the analysis of the data of the high-resolution powder neutron diffraction on $Pr_6Fe_{13}Ge$ compound without contamination of secondary phases, the following conclusions can be summarized.

1) Derived from Rietveld refinement, a second-order structural transition near 50 K is displayed by an anisotropic variation of lattice parameters a and c, with a magnetic phase transition. The magnetic coupling in the magnetic Pr_6Fe_{13} slabs is strongly ferromagnetic, whereas the inter-slab moments are collectively coupled antiferromagnetically with propagation vector $\boldsymbol{k}$=(001).

2) The temperature dependence of (110) diffraction intensity shows a strong similarity compared with the temperature-dependent magnetization, implying that there may be a small ferromagnetic component along the c-axis, although one cannot refine this magnetic component due to its low diffraction intensity.

3) In the practical magnetic structure of $Pr_6Fe_{13}Ge$, the small c-axis ferromagnetic component is combined with the dominant ab-plane interlayer antiferromagnetic structure. This spin configuration can give a self-consistent explanation to all contradictory experimental results, and is supported by the calculation of single ion anisotropy by the point charge model.

Acknowledgments

The authors wish to thank Dr Chang-Hee Lee of Neutron Physics Department, Korea Atomic Energy Research Institute for his kind help for the data collection, and Dr J. Rodriguez-Carvajal of Leon Brillouin Laboratory, France, for his informative discussion and critical reading.

References

[1] Weitzer F and Rogl P 1990 *J. Less-Common Metals* **167** 135
[2] Schrey P and Velicescu M 1991 *J. Magn. Magn. Mater.* **101** 417
[3] Cheng W H, Li W and Li C J 2001 *Acta Phys. Sin.* **50** 139 (in Chinese)
[4] Allemand J, Letant A, Moreau J M, Nozieres J P and de la Bathie R P 1990 *J. Less-Common Metals* **166** 73
[5] Sichevich O M, Lapunova R V, Sobolev A N, Grin Y N and Yarmolyuk Y P 1985 *Sov. Phys. Crystallogr.* **30** 627
[6] Yan Q *et al* 1994 *J. Phys.: Condens. Matter* **6** 3101
[7] de Groot C H, Buschow K H J and de Boer F R 1998 *Phys. Rev.* B **57** 11472
[8] Kajitani T, Nagayama K and Umeda T 1992 *J. Magn. Magn. Mater.* **117** 379
[9] Hu B P, Coey J M D, Klesnar H and Rogl P 1992 *J. Magn. Magn. Mater.* **117** 225
[10] Weitzer F, Leithe-Jasper A, Rogl P, Hiebl K, Rainbacher A, Wiesinger G, Steiner W, Friedl J and Wanger F E 1994 *J. Appl. Phys.* **75** 7745
[11] Wang F W, Zhang P L, Shen B G, Yan Q W and Gong H Y 2000 *J. Appl. Phys.* **87** 6043
[12] Jonen S and Rechenberg H R 1999 *J. Appl. Phys.* **85** 4448
[13] Schobinger-Papamantellos P, Buschow K H J, de Groot C H, de Boer F R, Ritter C, Fauth F and Boettger G 1998*J. Alloys Comp.* **280** 44
[14] Schobinger-Papamantellos P, Buschow K H J, de Groot C H, de Boer F R, Boettger G and Ritter C 1999 *J. Phys.: Condens. Matter* **11** 4469
[15] Kennedy S J, Wu E, Wang F W, Zhang P L and Yan Q W 2000 *Physica* B **276-278** 622
[16] Wang F W, Shen B G, Gong H Y, Sun X D, Zhang P L and Yan Q W 1998 *J. Magn. Magn. Mater.* **177-181** 1056
[17] Wang F W, Wang J Y, Zhang P L, Shen B G and Yan Q W 1999 *Physica* B **269** 17
[18] Xiao Q F, Zhao T, Zhang Z D, Yu M H, Zhao X G, Liu W, Geng D Y, Sun X K and de Boer F R 1998 *J. Magn. Magn. Mater.* **184** 330
[19] Wang F W, Zhang P L, Yan Q W and Gong H Y 2000 *Science in China* A **43** 1208
[20] Knoch K G, Le Calvez A, Qi Q, Leithe-Jasper A and Coey J M D 1993 *J. Appl. Phys.* **73** 5878
[21] Rodriguez-Carvajal J 1993 *Physica* B **192** 55
[22] Li H S, Hu B P, Cadogan J M, Coey J M D and Gavigan J P 1990 *J. Appl. Phys.* **67** 4841